

RESEARCH

Open Access



Determination of Sudan red contaminants at trace level from water samples by magnetic solid-phase extraction using Fe@NiAl-layered double hydroxide coupled with HPLC

Qingxiang Zhou^{*} , Yalin Wu, Yongyong Yuan, Xianqi Zhou, Hongyuan Wang, Yayan Tong, Yali Zhan^{*}, Yi Sun and Xueying Sheng

Abstract

Background: Sudan red dyes are widely used as color additions in various fields. Due to their potential carcinogenicity and large consumption, they have absorbed much more attention and become a research hot topic. There have been a few of existing methods for their analysis from samples; however, it is of great importance to develop simple, sensitive, and low-cost analytical method for public health and safety. This article described a new method based on magnetic Fe@NiAl-layered double hydroxides for enrichment of Sudan red dyes in combination with high-performance liquid chromatography.

Results: The as-prepared magnetic Fe@NiAl-layered double hydroxides (Fe@NiAl-LDHs) exhibited good adsorption capacity for Sudan red dyes, and could be used as an effective adsorbent for preconcentration of three Sudan Red dyes from environmental water samples. The proposed method provided low limits of detection in the range of 0.002–0.005 $\mu\text{g L}^{-1}$ with magnetic solid-phase extraction in combination with high-performance liquid chromatography.

Conclusion: The developed method utilized the easy to prepare magnetic materials as adsorbents and conventional analytical instrument and provided high sensitivity, which provided a robust and low consumption of toxic organic solvent alternative method. The results of present study are of great value for interested laboratories to monitor the level of Sudan red dyes in water samples or develop sensitive determination methods to monitor other pollutants at trace level in environmental waters.

Keywords: Sudan Red dyes, Fe@NiAl-layered double hydroxides, Magnetic solid-phase extraction, High-performance liquid chromatography

Background

Sudan Red dyes are lipophilic orange-red azo dyes [1, 2] and widely applied as color agents in various fields such as food, oils, waxes, shoe polishes, and plastics due to their simple synthetic method, low cost, and favorable availabilities [3–6]. Nevertheless, Sudan Red dyes are

regarded as category 3 carcinogenic by the International Agency for Research on Cancer (IARC) and can cause genetic mutations as well as cancer [7]. Many countries have banned the use of Sudan dyes as food additives [8, 9]. However, Sudan Red dyes are often found in food products as an additive to enhance the appearance of the food products such as chili powder, curry, chili sauces, curcuma, sausage, and so on [10–12]. Hence, it has become a hot topic attracting the public attention to detect and evaluate the safety of Sudan dyes.

*Correspondence: zhouqx@cup.edu.cn; ylzhan1970@163.com
State Key Laboratory of Heavy Oil Processing, College of Chemical Engineering and Environment, China University of Petroleum (Beijing), Beijing 102249, China

Until now, plenty of analytical methods have been developed for the determination of Sudan Red dyes such as fluorescence quenching [13], electrochemical methods [14, 15], surface-enhanced Raman scattering method [16, 17], capillary electrophoresis [18], high-performance liquid chromatography–mass spectrometry (LC–MS) [19], ultra-performance liquid chromatography–tandem mass spectrometry (UPLC–MS/MS) [20], high-performance liquid chromatography (HPLC) [21, 22], and so on. In general, it is difficult to directly analyze the target analytes because they are present in environment at low concentration and the sample matrix are complex. Hence it is of great value to develop simple and effective sample pretreatment technologies. At present, several sample pretreatment technologies have been established such as supercritical-fluid extraction, liquid–liquid microextraction, size-exclusion chromatography, solid-phase microextraction, solid-phase extraction, dispersive solid-phase extraction, and so on [23–34]. Among them, solid-phase extraction (SPE), an effective technology in environment sample pretreatment, has been widely used for the enrichment of environmental pollutants on account of its simplicity, good enrichment efficiency, and less consumption of toxic solvent [35].

Nowadays, magnetic solid-phase extraction (MSPE), a new mode of SPE, has absorbed more attention on a consequence of its favorable characteristics such as high extraction efficiency, simply separation, and saving time [36, 37]. It has been widely used for the preconcentration and detection of many environmental pollutants such as phenols, polycyclic aromatic hydrocarbons, 2,4,6-trinitrotoluene, and phthalate esters [38–41]. As an effective and promising pretreatment technique, magnetic nanoparticles (MNPs) are the core factor. In conventional MSPE, Fe_3O_4 is the often-used magnetic core of the adsorbent material and little attention has been put on nanoscale zero-valent iron (NZVI). Noticeably, NZVI has recently drawn scientific researchers' attention on account of its small particle size, high reactivity, and large surface area [42]. Nonetheless, the bare NZVI is unstable and easily oxidized, and so it is of great significance to modify surface to improve the stability of NZVI and increase the extraction efficiency.

During recent years, layered double hydroxides (LDHs), also named anionic clays, have drawn tremendous interest owing to its potential applications electrocatalysts, photocatalysts, adsorbents, ion-exchangers [43–46], etc. LDHs can be defined as the following formula $[\text{M(II)}_{1-x}\text{M(III)}_x(\text{OH})_2]^{x+}[\text{A}^{n-}]_{x/n} \cdot m\text{H}_2\text{O}$. M(II) represents divalent cations (Ca^{2+} , Mg^{2+} , Zn^{2+} , Mn^{2+} , Ni^{2+} , etc.), M(III) represents trivalent cations (Al^{3+} , Cr^{3+} , Fe^{3+} , etc.), A^{n-} represents interlayer anions (Cl^- , NO_3^- , ClO_4^- , CO_3^{2-} , etc.), respectively, while x is the molar ratio of M(III)/

[M(II) + M(III)] ranging from 0.17 to 0.33 [47, 48]. Structurally, LDHs consist of stacked brucite-like $\text{M}^{2+}(\text{OH})_2$ hydroxide layers. In the layers, some of the M^{2+} ions are replaced by M^{3+} ions through isomorphous substitutions. Anions are needed between adjacent layers to maintain charge neutrality [49]. The special structure of LDHs results in excellent properties including large surface area, high anionic exchange capability, high porosity, thermal stability, good dispersion [50], etc.

Up to now, there are few reports on the enrichment of Sudan dyes with LDHs. In this work, a novel composite Fe@NiAl-LDHs was synthesized to combine the merits of magnetic NZVI and NiAl-LDHs by a new two-step method. This composite possessed comprehensive advantages both easy separation of magnetic materials and large adsorption capacity of LDHs. The Fe@NiAl-LDHs were investigated as a MSPE adsorbent for the enrichment of Sudan Red II, Sudan Red III, and Sudan Red IV. The parameters influencing the extraction efficiency including eluent, amount of adsorbents, adsorption time, elution volume, elution time, pH, ionic strength, humic acid concentration, and sample volume were optimized.

Experimental

Materials and apparatus

Ferric chloride hexahydrate ($\text{FeCl}_3 \cdot 6\text{H}_2\text{O}$) was purchased from Sinopharm Chemical Reagent Co., Ltd (Shanghai, China). Hydrazine hydrate ($\text{N}_2\text{H}_4 \cdot \text{H}_2\text{O}$, >98%), Sudan Red II, Sudan Red III, and Sudan Red IV were obtained from Aladdin Chemistry Co., Ltd (Shanghai, China). Sodium hydroxide was obtained from Tianjin Guangfu Technology Development Co., Ltd (Tianjin, China). Sodium carbonate, ethanol, and acetone were obtained from Beijing Chemical Works (Beijing, China). Nickel nitrate hexahydrate ($\text{Ni}(\text{NO}_3)_2 \cdot 6\text{H}_2\text{O}$) and aluminum nitrate nonahydrate ($\text{Al}(\text{NO}_3)_3 \cdot 9\text{H}_2\text{O}$) were obtained from Beijing Yili Chemical Co., Ltd (Beijing, China). Methanol and acetonitrile (HPLC grade) were obtained from J&K Scientific Co., Ltd (Beijing, China). The deionized water was used in all experiments.

A high-performance liquid chromatography (HPLC) system (Shimadzu, Kyoto, Japan) equipped with a UV detector (SPD-20A) and a pump (LC-20AD) was used for analysis in all experiments. An Agilent InertSustain C18 (150×4.6 mm, $5 \mu\text{m}$) was used for separation and the mobile phase was acetonitrile with a flow rate of 1.0 mL min^{-1} . The detection wavelength was set at 520 nm and injection volume set at $20 \mu\text{L}$. Transmission electron microscopy (TEM) images were obtained with a JEM-2100 Transmission Electron Microscope (Japan). X-ray diffraction (XRD) was measured with a Bruker D8 Advance Diffractometer (Germany).

Synthesis of Fe@NiAl-LDHs

The Fe@NiAl-LDHs were prepared via a simple two-step method. Specifically, The Fe nanocubes were prepared according to a previous report with minor adjustment [51]. The preparation procedure was as follows: 2.4 g $\text{FeCl}_3 \cdot 6\text{H}_2\text{O}$ was dissolved in 12 mL ethanol, and 3.0 g NaOH and 4.8 mL $\text{N}_2\text{H}_4 \cdot \text{H}_2\text{O}$ were added into the reactor under vigorous mechanical stirring. Then, the mixture was sealed in a 50 mL autoclave and heated at 80 °C for 10 h. After that, cooled to room temperature, the particulate materials were collected by a magnet and washed with water and ethanol for several times. Finally, the obtained materials were dried in vacuum at 50 °C overnight.

The Fe@NiAl-LDHs were synthesized by co-precipitation method. 300 mg Fe nanotubes, 812 mg $\text{Ni}(\text{NO}_3)_2 \cdot 6\text{H}_2\text{O}$, and 525 mg $\text{Al}(\text{NO}_3)_3 \cdot 9\text{H}_2\text{O}$ were dissolved in 100 mL deionized water and the mixture was ultrasonically for 20 min. Then a mixed solution containing NaOH and Na_2CO_3 was added dropwise into the above-mentioned mixture under vigorous mechanical stirring to adjust the pH at about 10. After that, the solution was stirred for another 2 h at 60 °C. Eventually, the black powders were collected by a magnet and washed with deionized water for several times and dried in vacuum at 50 °C overnight.

MSPE procedure

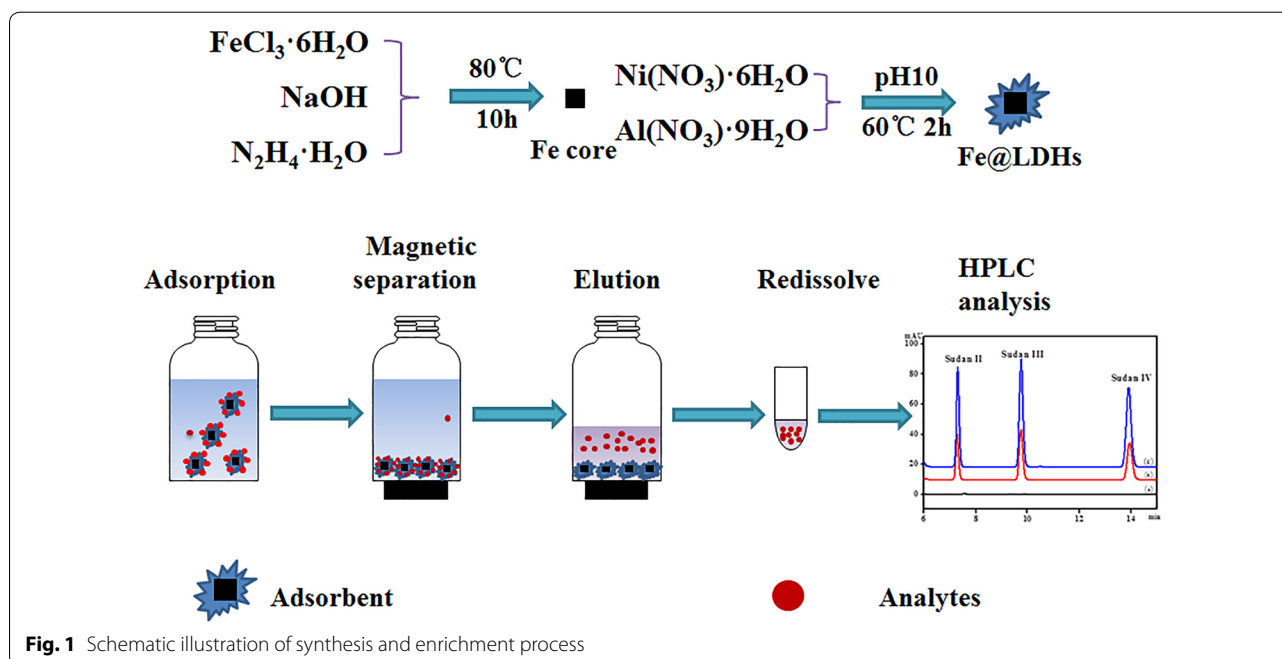
First of all, 50 mg Fe@NiAl-LDHs nanoparticles were dispersed into 50 mL deionized water containing target

compounds at a concentration of $10 \mu\text{g L}^{-1}$. The suspension was stirred for 1 h. Secondly, the adsorbent was separated from liquid phase via putting a magnet under the bottom of the beaker and the supernatant was taken out. Then, the target contaminants were eluted for 9 min from the adsorbent with 6 mL acetone. After that, the eluent was separated by a magnet and blown to near dryness with nitrogen gas flow. Eventually, the residue was redissolved in 200 μL methanol, and 20 μL was injected into HPLC for analysis. The whole experimental procedure is shown in the following Fig. 1.

Results and discussion

Characterization of Fe@NiAl-LDHs

Figure 2a shows the TEM image and corresponding EDS spectrum of Fe@NiAl-LDHs. As revealed by the image, Fe nanocubes were about 300 nm in diameter. The surface of Fe nanoparticles was uniformly covered with NiAl-LDHs and its diameter was about 350–400 nm. The element composition of material was analyzed by EDS. As can be seen from Fig. 2a, the material contained N, O, Al, Fe, and Ni elements. Figure 2b displayed the XRD patterns of NiAl-LDHs, Fe^0 , and Fe@NiAl-LDHs. For NiAl-LDHs, four evident diffraction peaks at about $2\theta = 11.3^\circ, 23.2^\circ, 35.5^\circ,$ and 61.7° were similar to a previous report [52]. As Fe^0 was concerned, three obvious diffraction peaks were at about $2\theta = 44.8^\circ, 65.2^\circ,$ and 82.7° , which was quite consistent with a previous study [51]. Diffraction Peaks of iron oxides or hydroxides were undetected. Thus, Fe^0 was



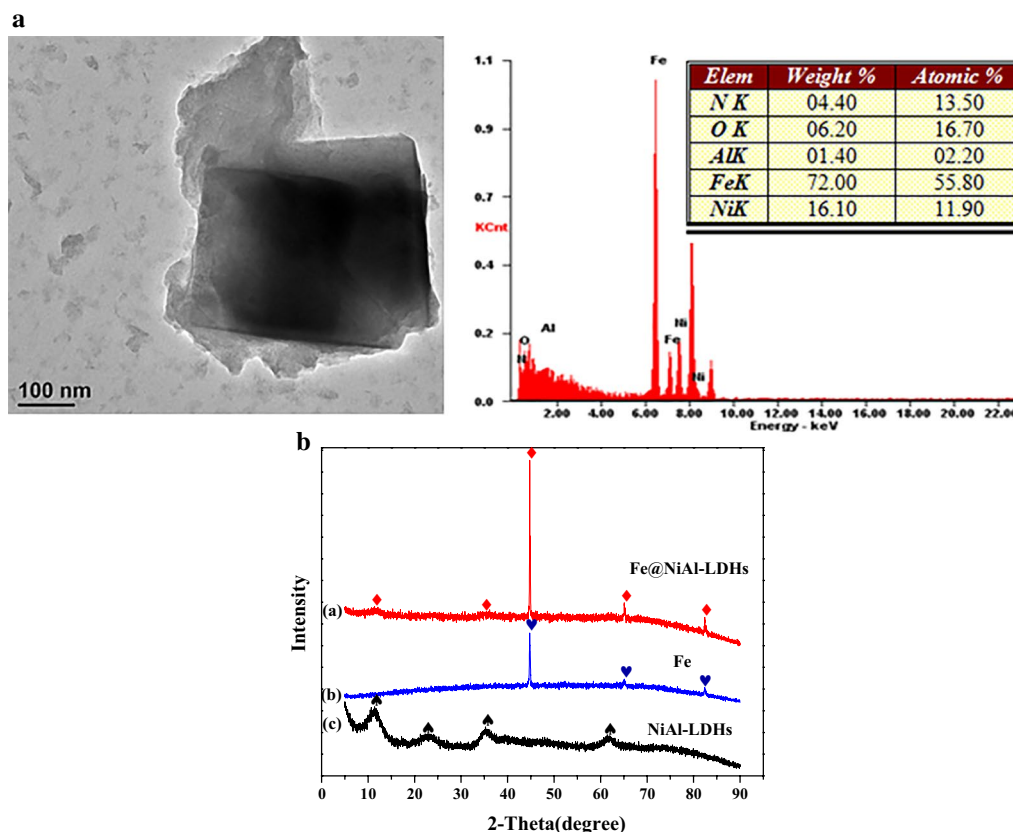


Fig. 2 **a** TEM and EDS images of Fe@NiAl-LDHs nanoparticles; **b** XRD patterns of (a) Fe@NiAl-LDHs, (b) Fe⁰, and (c) NiAl-LDHs

synthesized as expected. For Fe@NiAl-LDHs nanoparticles, five remarkable diffraction peaks at about $2\theta = 11.3^\circ, 35.5^\circ, 44.8^\circ, 65.2^\circ,$ and 82.7° illustrated that NiAl-LDHs were successfully coated on the surface of Fe nanocubes. Diffraction peaks at about $2\theta = 23.2^\circ$ and 61.7° were not obvious. The possible reason was that the two diffraction peaks were too weak in comparison with the diffraction peaks of Fe⁰. These data demonstrated that magnetic Fe@NiAl-LDHs nanoparticles were successfully prepared.

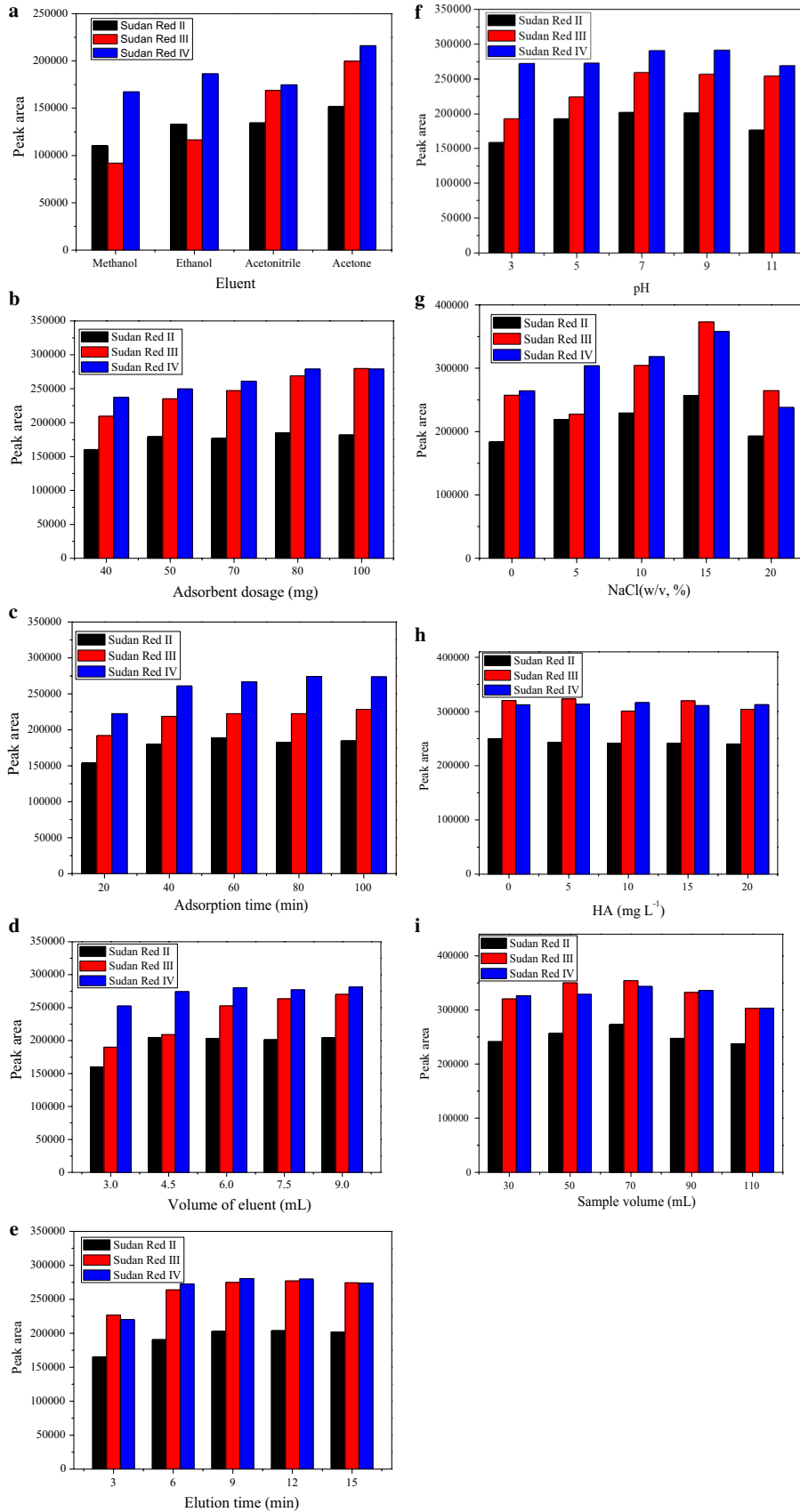
Optimization of MSPE

Eluent plays an important role in the procedure of MSPE. It is crucial to choose the best eluent because the physical and chemical properties of different organic solvents

will put a profound effect on the elution efficiency. In order to achieve much higher elution efficiency, four eluent solvents including methanol, ethanol, acetone and acetonitrile were investigated. The results were shown in Fig. 3a. It was obviously that four organic solvents resulted in different preconcentration performance, and the largest peak area was obtained with acetone as the eluent. The enrichment performance of ethanol was better than that of methanol. As acetonitrile was concerned, it resulted in better performance for Sudan Red III, similar performance for Sudan Red I and poor performance for Sudan IV than that with ethanol as the eluent. The reason may be that the polarity of acetone is the smallest among the four solvents, and the polarity of the three Sudan Red dyes is very poor and which make them have

(See figure on next page.)

Fig. 3 Optimization of enrichment parameters. **a** Selection of the eluent; **b** Effect of the Fe@NiAl-LDHs dosage; **c** Effect of the adsorption time; **d** Effect of the volume of eluent; **e** Effect of the elution time; **f** Effect of the sample pH; **g** Effect of the ionic strength; **h** Effect of the humic acid; **i** Selection of the sample volume. Experimental conditions: spiked level of analytes, $10 \mu\text{g L}^{-1}$; Fe@NiAl-LDHs amount, 50 mg; adsorption time, 60 min; elution volume, 6 mL; elution time, 9 min; pH, 7; concentration of NaCl, 0% (w/v); concentration of humic acid, 0 mg L^{-1} ; sample volume, 50 mL. For each parameter, it was optimized with other parameters keeping constant, and the optimal value was used after optimization



higher solubility in acetone based the principle of similarity. Therefore, acetone was chosen for use in subsequent experiments.

In general, the dosage of adsorbent is one of the most important factors which influence the enrichment efficiency, and which was investigated in the range of 40–100 mg. Figure 3b shows that the enrichment efficiency increased with the increase of adsorbent dosage, and the largest peak area of all analytes was achieved when 80 mg adsorbent was used. After that, the enrichment efficiency changed very little with continuous increase of the adsorbent dosage. This may contribute to the fact that the increase of adsorbent dosage resulted in the increase of the active adsorption sites, and further led to the increase of the adsorbed amount of analytes. However, it got equilibrium between adsorbent and target contaminants when the adsorbent dosage increased to 80 mg. With the continuous increase of adsorbent dosage, the enrichment performance will keep the constant. Hence, 80 mg adsorbent was used in the following experiments.

Adsorption time is another significant factor affecting the enrichment process. In order to investigate the effect of adsorption time, adsorption time was investigated in the range of 20–100 min. As shown in Fig. 3c, the peak area increased with the increase of adsorption time up to 60 min and kept constant when the adsorption time was over 60 min. In order to achieve best enrichment efficiency as well as saving time, 60 min was used in the following experiments.

In the elution procedure, both volume of eluent and elution time are two important factors, which were optimized in the range of 3–9 mL and 3–15 min, respectively. The results were exhibited in Fig. 3d, e. From the two figures, it was found that the maximum peak area was obtained with 7.5 mL eluent eluting for 9 min. Afterwards, the peak area changed very few with the increase of eluent volume and elution time.

It is known that sample pH is vital in MSPE process, because it can affect the existing states of adsorbent and analytes, and further affect the enrichment performance. Sample pH was optimized in the range of pH 3–11. Figure 3f shows that largest peak area of the analytes was achieved at pH 7. There was a definite possibility that the adsorbent was dissolved under acidic condition and the structure of NiAl-LDHs was broken when the pH was lower than pH 7, while the pH was at a higher value, the target contaminants were easy to be ionized and the

solubility of analytes in water increased. Hence pH 7 was used in the followed experiments.

Generally, the solubility of analyte is easily influenced by ionic strength of the solution. For this reason, we can change ionic strength to lower the solubility of target contaminant to improve the adsorption efficiency. A series of experiments were designed to investigate the effect of ionic strength on adsorption efficiency at five levels in the range of 0–20% (w/v) with the addition of NaCl to adjust the ionic strength of solution. The results are shown in Fig. 3g. Figure 3g shows that the peak areas of analytes increased with the increase of NaCl concentration from 0 to 15%. The reason may be that the addition of NaCl led to the salting-out effect, which decreased the solubility of Sudan dyes in aqueous solution. The enrichment efficiency decreased with the concentration of NaCl increasing to 20%, which may be due to the fact that the viscosity of solution increased which decreased the migration rate of the analytes onto the surface of adsorbent and less of target analytes were adsorbed onto the adsorbent in the same time interval. Hence, the concentration of NaCl was set at 15% (w/v).

Humic acid is usually present in almost all nature waters. The existence of humic acid may cause a certain influence on the adsorption of analytes by competitive adsorption. A series of concentrations of humic acid in the range of 0–20 $\mu\text{g mL}^{-1}$ were investigated. Figure 3h illustrates that the peak areas of analytes had no obvious change with different concentrations of humic acid. It was very probable that adsorbent had stronger adsorption capacity to Sudan dyes than humic acid. Therefore, no humic acid was added in order to save time.

Sample volume is also an important factor for achieving higher sensitivity. In this experiment, sample volume was optimized in the range from 30 to 110 mL and the result is shown in Fig. 3i. It was found that the peak areas of analytes had a slight increase as the sample volume increased from 30 to 70 mL. After that, the peak areas decreased as the sample volume increased from 70 to 110 mL, which was due to that the amount of adsorbent per volume decreased and the migration distance to the surface of adsorbent increased, which led to the decrease of peak areas in limited time. Therefore, 70 mL was utilized in later experiments.

Analytical performance of the proposed method

Under the optimal experimental conditions, analytical parameters of this proposed method including linearity,

Table 1 Analytical parameters of method

Compounds	Regression equation	Linear range ($\mu\text{g L}^{-1}$)	R^2	Precisions (% , $n=6$)	LOD ($\mu\text{g L}^{-1}$)
Sudan II	$y=31080x-53102$	0.01–300	0.997	2.81	0.004
Sudan III	$y=39097x+3167.6$	0.01–300	0.999	1.21	0.002
Sudan IV	$y=39975x-15884$	0.01–300	0.999	5.07	0.005

Table 2 Analytical results in real water samples

Water sample	Spiked ($\mu\text{g L}^{-1}$)	Recovery (%)		
		Sudan II	Sudan III	Sudan IV
Changping Park water	0	nd	nd	nd
	5	$104.8^a \pm 2.8^b$	99.3 ± 0.6	100.9 ± 2.8
	10	97.8 ± 2.7	98.7 ± 0.05	99.6 ± 1.7
Ming Tombs Reservoir	0	nd ^c	nd	nd
	5	98.9 ± 2.0	100.3 ± 0.1	101.2 ± 2.0
	10	105.7 ± 2.7	99.8 ± 3.8	100.4 ± 4.4
Binhe Park water	0	nd	nd	nd
	5	97.6 ± 3.6	100.7 ± 4.2	102.4 ± 4.5
	10	100.6 ± 2.5	103.1 ± 4.9	101.8 ± 3.6

^a Mean of three determinations

^b Standard deviation for three determinations

^c Not detected

limits of detection, and precisions were investigated. The results are listed in Table 1. Excellent linearity was observed in the range of 0.01–300 $\mu\text{g L}^{-1}$ with good correlation coefficients ($r^2 \geq 0.997$) for three Sudan dyes. The limits of detection (LOD, $S/N=3$) were 0.004 $\mu\text{g L}^{-1}$ for Sudan Red II, 0.002 $\mu\text{g L}^{-1}$ for Sudan Red III, and 0.005 $\mu\text{g L}^{-1}$ for Sudan Red IV, respectively. The precisions (RSD, $n=6$) were 2.81% for Sudan Red II, 1.21% for Sudan Red III, and 5.07% for Sudan Red IV, respectively.

Real sample analysis

The proposed method was evaluated with three different natural water samples including Changping Park water, Ming Tombs Reservoir water, and Binhe Park water. The results are listed in Table 2 and the typical chromatograms of water samples are shown in Fig. 4. Sudan dyes were not detected in all three natural water samples. The mean spiked recoveries were all in the range of 97.6–105.7%. Besides, the proposed method was compared with other previous reported methods for the enrichment and determination of Sudan dyes from the viewpoint of linearity range and LOD. The results are depicted in Table 3. It is obvious that present method possessed wider linearity range and lower LODs. Based on the experimental results, the developed method based on Fe@NiAl-LDHs had good practicability in the enrichment and determination of Sudan Red contaminants in water samples.

Conclusion

In present work, Fe@NiAl-LDHs, a kind of novel magnetic nanoparticles, was firstly synthesized and used in magnetic solid-phase extraction prior to HPLC–UV for the enrichment and determination of Sudan dyes in environmental water samples. The developed method provided an excellent linearity in the range of 0.01–300

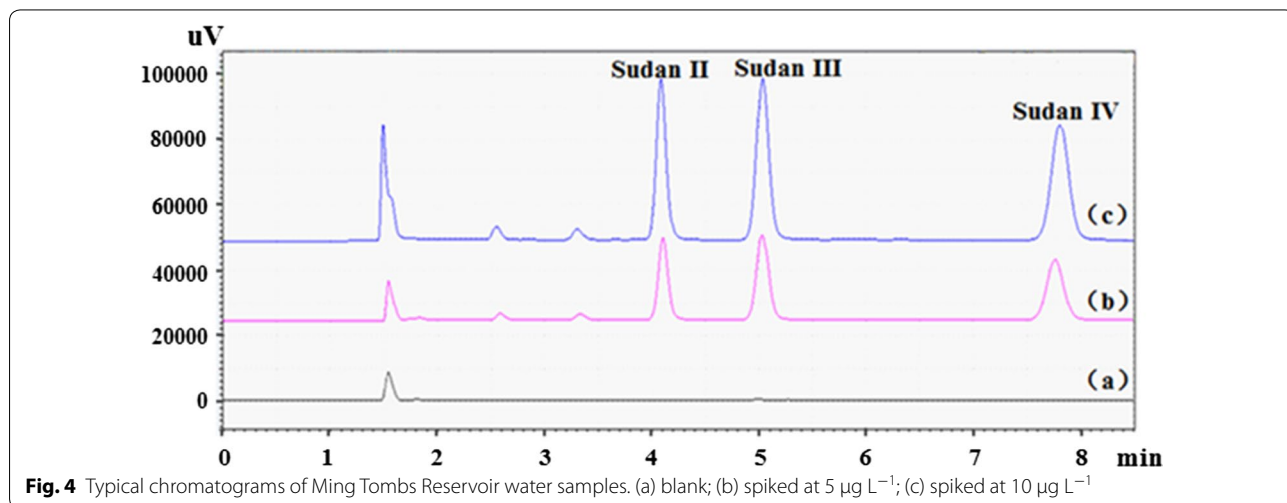


Fig. 4 Typical chromatograms of Ming Tombs Reservoir water samples. (a) blank; (b) spiked at 5 $\mu\text{g L}^{-1}$; (c) spiked at 10 $\mu\text{g L}^{-1}$

Table 3 Comparison with reported methods for the Sudan dyes determination

Sample pretreatment method	Detection method	Matrices	Linear ranges ($\mu\text{g L}^{-1}$)			LOD ($\mu\text{g L}^{-1}$)	Refs.
			Sudan II	Sudan III	Sudan IV		
MSPE	HPLC	Water	0.025–5	0.025–5	0.025–5	0.0029–0.0068	[4]
MSPE	UFLC ^a	Juice	0.0208–15	0.0208–15	0.0625–15	0.0057–0.017	[5]
MSPE	Capillary LC	Food	0.25–2	0.25–2	0.25–2	0.05–0.07	[18]
DLLME ^b	HPLC	Water	0.3–40	1.2–160	1.2–160	0.18–0.46	[21]
MA-LLME ^c	HPLC	Juice	4.5–300	4.50–250	4.50–250	1.14–1.30	[53]
MSPE	HPLC	Water	0.1–300	0.1–300	0.1–300	0.002–0.005	Present work

^a Ultrafast liquid chromatography

^b Dispersive liquid–liquid microextraction

^c Microwave-assisted liquid–liquid microextraction

$\mu\text{g L}^{-1}$ and low LODs in the range of 0.002–0.005 $\mu\text{g L}^{-1}$ for three Sudan dyes. Fe@NiAl-LDHs exhibited excellent enrichment capability to Sudan Red dyes and the developed MSPE-HPLC method possessed advantages such as simplicity, fastness, easy to separate, and high enrichment efficiency compared with other previous methods, which can match the demand of determining trace Sudan dyes in natural water samples, and would be a good alternative tool for the enrichment and detection of Sudan dyes contaminants in environmental water samples.

Abbreviations

Fe@NiAl-LDHs: Fe@NiAl-layered double hydroxides; HPLC: high-performance liquid chromatography; IARC: international agency for research on cancer; LC-MS: high-performance liquid chromatography–mass spectrometry; UPLC-MS/MS: ultra-performance liquid chromatography–tandem mass spectrometry; SPE: solid-phase extraction; MSPE: magnetic solid-phase extraction; MNPs: magnetic nanoparticles; NZVI: nanoscale zero-valent iron; LDHs: layered double hydroxides; LOD: limits of detection; HPLC-UV: high-performance liquid chromatography-ultraviolet detector; MSPE-HPLC: magnetic solid-phase extraction-high-performance liquid chromatography; DLLME: dispersive liquid–liquid microextraction; MA-LLME: microwave-assisted liquid–liquid microextraction; UFLC: ultrafast liquid chromatography.

Acknowledgements

Not applicable.

Authors' contributions

YW contributed to the experimental studies, data acquisition, analysis, manuscript preparation, and editing. YW and YZ contributed to the experimental design. QZ and YZ are the guarantor of integrity of the entire study and contributed to the study concepts and design, manuscript revision/review, and manuscript's final version approval. YY, XZ, HW, YT, YS, and XS contributed to the experimental discussion. All authors read and approved the final manuscript.

Funding

The work was supported by the National Natural Science Foundation of China (21377167, 21677177).

Availability of data and materials

Not applicable.

Ethics approval and consent to participate

Not applicable.

Consent for publication

All authors agreed to publish the paper.

Competing interests

The authors declare that they have no competing interests.

Received: 8 April 2019 Accepted: 10 May 2019

Published online: 27 May 2019

References

- Berlina AN, Zherdev AV, Xu C, Eremin SA, Dzantiev BB (2017) Development of lateral flow immunoassay for rapid control and quantification of the presence of the colorant Sudan I in spices and seafood. *Food Control* 73:247–253
- Petrakis EA, Cagliani LR, Tarantilis PA, Polissiou MG, Consonni R (2017) Sudan dyes in adulterated saffron (*Crocus sativus* L.): identification and quantification by ¹H NMR. *Food Chem* 217:418–424
- Prabakaran E, Pandian K (2015) Amperometric detection of Sudan I in red chili powder samples using Ag nanoparticles decorated graphene oxide modified glassy carbon electrode. *Food Chem* 166:198–205
- Li C, Chen L, You X (2014) Extraction of Sudan dyes from environmental water by hemimicelles-based magnetic titanium dioxide nanoparticles. *Environ Sci Pollut Res* 21:12382–12389
- Yu X, Sun Y, Jiang CZ, Gao Y, Wang YP, Zhang HQ, Song DQ (2012) Magnetic solid-phase extraction and ultrafast liquid chromatographic detection of Sudan dyes in red wines, juices, and mature vinegars. *J Sep Sci* 35:3403–3411
- Xie X, Chen L, Pan X, Wang S (2015) Synthesis of magnetic molecularly imprinted polymers by reversible addition fragmentation chain transfer strategy and its application in the Sudan dyes residue analysis. *J Chromatogr A* 1405:32–39
- Ávila M, Zougagh M, Escarpa A, Ríos Á (2011) Determination of Sudan dyes in food samples using supercritical fluid extraction–capillary liquid chromatography. *J Supercrit Fluids* 55:977–982
- Qiao F, Geng Y, He C, Wu Y, Pan P (2011) Molecularly imprinted microspheres as SPE sorbent for selective extraction of four Sudan dyes in catsup products. *J Chromatogr B* 879:2891–2896
- Pardo O, Yusa V, Leon N, Pastor A (2009) Development of a method for the analysis of seven banned azo-dyes in chilli and hot chilli food samples by pressurised liquid extraction and liquid chromatography with electrospray ionization–tandem mass spectrometry. *Talanta* 78:178–186
- Schummer C, Sassel J, Bonenberger P, Moris G (2013) Low-level detections of Sudan I, II, III and IV in spices and chili-containing foodstuffs using UPLC-ESI-MS/MS. *J Agric Food Chem* 61:2284–2289
- Yan H, Qiao J, Wang H, Yang G, Row KH (2011) Molecularly imprinted solid-phase extraction combined with ultrasound-assisted dispersive liquid–liquid microextraction for the determination of four Sudan dyes in sausage samples. *Analyst* 136:2629–2634

12. Jiang C, Sun Y, Yu X, Zhang L, Sun X, Gao Y, Zhang H, Song D (2012) Removal of Sudan dyes from water with C_{18} -functional ultrafine magnetic silica nanoparticles. *Talanta* 89:38–46
13. Fang A, Long Q, Wu Q, Li H, Zhang Y, Yao S (2016) Upconversion nanosensor for sensitive fluorescence detection of Sudan I–IV based on inner filter effect. *Talanta* 148:129–134
14. Ma X, Chao M, Wang Z (2013) Voltammetric determination of Sudan II in food samples at graphene modified glassy carbon electrode based on the enhancement effect of sodium dodecyl sulfate. *J Chem Soc Pakistan* 138:739–744
15. Heydari M, MehdiGhoreishi S, Khoobi A (2019) Chemometrics-assisted determination of Sudan dyes using zinc oxide nanoparticle-based electrochemical sensor. *Food Chem* 283:68–72
16. Deng DD, Yang H, Liu C, Zhao K, Li JG, Deng AP (2019) Ultrasensitive detection of Sudan I in food samples by a quantitative immunochromatographic assay. *Food Chem* 277:595–603
17. Wu MM, Li P, Zhu QX, Wu MR, Li H, Lu F (2018) Functional paper-based SERS substrate for rapid and sensitive detection of Sudan dyes in herbal medicine. *Spectrochim Acta A Mol Biomol Spectrosc* 196:110–116
18. Benmassaoud Y, Villasenor MJ, Salghi R, Jodeh S, Algarra M, Zougagh M, Rios A (2017) Magnetic/non-magnetic argan press cake nanocellulose for the selective extraction of Sudan dyes in food samples prior to the determination by capillary liquid chromatography. *Talanta* 166:63–69
19. Chen D, Li X, Tao Y, Pan Y, Wu Q, Liu Z, Peng D, Wang X, Huang L, Wang Y, Yuan Z (2013) Development of a liquid chromatography–tandem mass spectrometry with ultrasound-assisted extraction method for the simultaneous determination of Sudan dyes and their metabolites in the edible tissues and eggs of food-producing animals. *J Chromatogr B* 939:45–50
20. Hou X, Li Y, Cao S, Zhang Z, Wu Y (2009) Analysis of para red and Sudan dyes in egg yolk by UPLC–MS–MS. *Chromatographia* 71:135–138
21. Zhou Q, Zhao K, Xing A (2014) Dispersive liquid–liquid microextraction combined with high-performance liquid chromatography for the enrichment and sensitive determination of Sudan Red pollutants in water samples. *J Sep Sci* 37:3347–3353
22. Ji W, Zhang M, Wang T, Wang X, Zheng Z, Gong J (2017) Molecularly imprinted solid-phase extraction method based on SH-Au modified silica gel for the detection of six Sudan dyes in chili powder samples. *Talanta* 165:18–26
23. da Silva RPPF, Rocha-Santos TAP, Duarte AC (2016) Supercritical fluid extraction of bioactive compounds. *Trends Anal Chem* 76:40–51
24. Wang ZF, Cui ZJ (2016) Supercritical fluid extraction and gas chromatography analysis of arsenic species from solid matrices. *Chin Chem Lett* 27:241–246
25. Zhang R, Cheng X, Guo J, Zhang H, Hao X (2017) Comparison of two ionic liquid-based pretreatment methods for three steroids' separation and determination in water samples by HPLC. *Chromatographia* 80:237–246
26. Wang H, Levi MS, Del Grosso AV, McCormick WM, Bhattacharyya L (2017) An improved size exclusion-HPLC method for molecular size distribution analysis of immunoglobulin G using sodium perchlorate in the eluent. *J Pharm Biomed Anal* 138:330–343
27. Ran C, Chen D, Xu M, Du C, Li Q, Jiang Y (2016) A study on characteristic of different sample pretreatment methods to evaluate the entrapment efficiency of liposomes. *J Chromatogr B* 1028:56–62
28. Feng Y, Su G, Sun-Waterhouse D, Cai Y, Zhao H, Cui C, Zhao M (2016) Optimization of headspace solid-phase micro-extraction (HS-SPME) for analyzing soy sauce aroma compounds via coupling with direct GC–olfactometry (D-GC-O) and gas chromatography–mass spectrometry (GC-MS). *Food Anal Methods* 10:713–726
29. Ran C, Chen D, Ma H, Jiang Y (2017) Graphene oxide adsorbent based dispersive solid phase extraction coupled with multi-pretreatment clean-up for analysis of trace aflatoxins in traditional proprietary Chinese medicines. *J Chromatogr B* 1044–1045:120–126
30. Ma JQ, Liu L, Wang X, Chen LZ, Lin JM, Zhao RS (2019) Development of dispersive solid-phase extraction with polyphenylene conjugated microporous polymers for sensitive determination of phenoxy-carboxylic acids in environmental water samples. *J Hazard Mater* 371:433–439
31. Liu L, Meng WK, Li L, Xu GJ, Wang X, Chen LZ, Wang ML, Lin JM, Zhao RS (2019) Facile room-temperature synthesis of a spherical mesoporous covalent organic framework for ultrasensitive solid-phase microextraction of phenols prior to gas chromatography–tandem mass spectrometry. *Chem Eng J* 369:920–927
32. Liu L, Meng WK, Zhou YS, Wang X, Xu GJ, Wang ML, Lin JM, Zhao RS (2019) β -Ketoenamine-linked covalent organic framework coating for ultra-high-performance solid-phase microextraction of polybrominated diphenyl ethers from environmental samples. *Chem Eng J* 356:926–933
33. Zhang BB, Xu GJ, Li L, Wang XL, Li N, Zhao RS, Lin JM (2018) Facile fabrication of MIL-96 as coating fiber for solid-phase microextraction of trihalomethanes and halonitromethanes in water samples. *Chem Eng J* 350:240–247
34. Bazregar M, Rajabi M, Yamini Y, Arghavani-Beydokhti S, Asghari A (2018) Centrifugeless dispersive liquid–liquid microextraction based on salting-out phenomenon followed by high performance liquid chromatography for determination of Sudan dyes in different species. *Food Chem* 244:1–6
35. Omid F, Behbahani M, Bojdi MK, Shahtaheri SJ (2015) Solid phase extraction and trace monitoring of cadmium ions in environmental water and food samples based on modified magnetic nanoporous silica. *J Magn Magn Mater* 395:213–220
36. Li N, Chen J, Shi YP (2016) Magnetic reduced graphene oxide functionalized with beta-cyclodextrin as magnetic solid-phase extraction adsorbents for the determination of phytohormones in tomatoes coupled with high performance liquid chromatography. *J Chromatogr A* 1441:24–33
37. Li N, Jiang HL, Wang XL, Wang X, Xu GJ, Zhang BB, Wang LJ, Zhao RS, Lin JM (2018) Recent advances in graphene-based magnetic composites for magnetic solid-phase extraction. *TRAC Trends Anal Chem* 102:60–74
38. Gong SX, Wang XL, Liu W, Wang ML, Wang X, Wang ZW, Zhao RS (2017) Aminosilanized magnetic carbon microspheres for the magnetic solid-phase extraction of bisphenol A, bisphenol AF, and tetrabromobisphenol A from environmental water samples. *J Sep Sci* 40:1755–1764
39. Zhou Q, Lei M, Wu Y, Yuan Y (2017) Magnetic solid phase extraction of typical polycyclic aromatic hydrocarbons from environmental water samples with metal organic framework MIL-101 (Cr) modified zero valent iron nano-particles. *J Chromatogr A* 1487:22–29
40. Costa Dos Reis L, Vidal L, Canals A (2017) Graphene oxide/ Fe_3O_4 as sorbent for magnetic solid-phase extraction coupled with liquid chromatography to determine 2,4,6-trinitrotoluene in water samples. *Anal Bioanal Chem* 409:2665–2674
41. Liu X, Sun Z, Chen G, Zhang W, Cai Y, Kong R, Wang X, Suo Y, You J (2015) Determination of phthalate esters in environmental water by magnetic zeolitic imidazolate framework-8 solid-phase extraction coupled with high-performance liquid chromatography. *J Chromatogr A* 1409:46–52
42. Zhou Q, Lei M, Li J, Zhao K, Liu Y (2016) Determination of 1-naphthol and 2-naphthol from environmental waters by magnetic solid phase extraction with $Fe@MgAl$ -layered double hydroxides nanoparticles as the adsorbents prior to high performance liquid chromatography. *J Chromatogr A* 1441:1–7
43. Youn DH, Park YB, Kim JY, Magesh G, Jang YJ, Lee JS (2015) One-pot synthesis of NiFe layered double hydroxide/reduced graphene oxide composite as an efficient electrocatalyst for electrochemical and photoelectrochemical water oxidation. *J Power Sources* 294:437–443
44. Iguchi S, Kikkawa S, Teramura K, Hosokawa S, Tanaka T (2016) Investigation of the electrochemical and photoelectrochemical properties of Ni–Al LDH photocatalysts. *Phys Chem Chem Phys* 18:13811
45. Li Y, Bi HY, Jin YS (2017) Facile preparation of rhamnolipid-layered double hydroxide nanocomposite for simultaneous adsorption of p-cresol and copper ions from water. *Chem Eng J* 308:78–88
46. Kang G, Zhu Z, Tang BH, Wu CH, Wu RJ (2017) Rapid detection of ozone in the parts per billion range using a novel Ni–Al layered double hydroxide. *Sens Actuators B Chem* 241:1203–1209
47. Yu S, Wang J, Song S, Sun K, Li J, Wang X, Chen Z, Wang X (2017) One-pot synthesis of graphene oxide and Ni–Al layered double hydroxides nanocomposites for the efficient removal of U(VI) from wastewater. *Sci China Chem* 60:415–422
48. Barnabas MJ, Parambadath S, Mathew A, Park SS, Vinu A, Ha CS (2016) Highly efficient and selective adsorption of In^{3+} on pristine Zn/Al layered double hydroxide (Zn/Al-LDH) from aqueous solutions. *J Solid State Chem* 233:133–142
49. Nayak S, Parida KM (2016) Nanostructured $CeO_2/MgAl$ -LDH composite for visible light induced water reduction reaction. *Int J Hydrogen Energy* 41:21166–21180
50. Mallakpour S, Dinari M (2015) Effect of organically modified Ni–Al layered double hydroxide loading on the thermal and morphological properties

of L-methionine containing poly(amide-imide) nanocomposites. *RSC Adv* 5:28007–28013

51. Qi B, Li D, Ni X, Zheng H (2007) A facile chemical reduction route to the preparation of single-crystalline iron nanocubes. *Chem Lett* 36:722–723
52. Kameda T, Kondo E, Yoshioka T (2015) Treatment of Cr(VI) in aqueous solution by Ni–Al and Co–Al layered double hydroxides: equilibrium and kinetic studies. *J Water Process Eng* 8:e75–e80
53. Hu M, Wu L, Song Y, Li Z, Ma Q, Zhang H, Wang Z (2016) Determination of Sudan Dyes in juice samples via solidification of ionic liquid in microwave-assisted liquid–liquid microextraction followed by high-performance liquid chromatography. *Food Anal Methods* 9:2124–2132

Publisher's Note

Springer Nature remains neutral with regard to jurisdictional claims in published maps and institutional affiliations.

Submit your manuscript to a SpringerOpen[®] journal and benefit from:

- Convenient online submission
- Rigorous peer review
- Open access: articles freely available online
- High visibility within the field
- Retaining the copyright to your article

Submit your next manuscript at ► [springeropen.com](https://www.springeropen.com)
